Study of Barium Hexaferrite ($BaFe_{12}O_{19}$) Synthesised by Sol Gel Auto-Combustion Technique

A thesis submitted in partial fulfilment of the requirement for the degree of

MASTER OF SCIENCE

IN

PHYSICS

by

NiloferParween

Roll No-412PH2107

Under the Guidance

Of

Prof-S.Panigrahi

DEPT OF PHYSICS AND ASTRONOMY

National Institute of Technology, Rourkela

Prof S.Panigrahi

Dept. of Physics and Astronomy

National institute of technology

Rourkela-769001

National Institute of Technology, Rourkela

CERTIFICATE

This is to certify that the thesis entitled **"*Study of Barium Hexaferrite ($BaFe_{12}O_{19}$) Synthesised by Sol Gel Auto-Combustion Technique*"** submitted by NiloferParween on partial fulfilment for the requirement for the award of degree in Master of science in physics, National institute of technology, Rourkela is an authentic work carried out by her under my supervision and guidance.

To the best of my knowledge, the matter embodied in this project has not been submitted to any other university or institute for the award of any degree or diploma.

Place: Signature of the guide

Date: (Prof S.Panigrahi)

ACKNOWLEDGEMENT

I take this opportunity to express my profound gratitude and deep regards to my guide Prof.S.Panigrahi for his exemplary guidance, monitoring and constant encouragement throughout the course of this one year project .The blessing,help and guidance given by him time to time shall carry me a long way in the journey of life on which I am about to embark.

I also take the opportunity to express a deep sense of gratitude to our Ph.d. scholars RakeshMuduli, RanjeetPattanaik and PriyambadaNayak for their cordial support, valuable information and guidance which helped me completing this task through various stages..

Lastly, I thanks to the almighty, my parent and brother for their constant encouragement without which this assignment would not be possible.

ABSTRACT

The powders of barium ferrite ($BaFe_{12}O_{19}$) were synthesized from metal nitrates in the molar ratio of 1:9:10 (Ba/Fe/glycine) by a sol–gel auto combustion technique using glycine as firing agent. At the time of synthesis three types of precautions considered such as, without considering any extra agent (Sample-1), the solution maintained the Ph value 7 by adding ammonia solution (Sample-2) and by adding nitric acid (Sample-3). All the combusted samples calcined at different temperatures and time durations for confirmation of phase formation. The XRD study of calcined samples reveals the single phase formation of $BaFe_{12}O_{19}$ but for different precautions the phase formation temperatures and time durations are different. It is found that the calcined temperature for Sample-1 is 1000^{o}C/3hr, for Sample-2 it is 950^{o}C /3hr and for Sample-3 it is 950^{o}C/5hr. Particle size for all the calcined samples measured by Scherrer formula. The UV-Visible spectroscopy of all samples studied and the measured band gap of all samples form UV-Visible data. For Sample-2 room temperature Dielectric and impedance spectroscopy study done by WK LCR meter.

TABLE OF CONTENTS

CONTENTS **PAGE NO.**

LIST OF FIGURES PAGE NO.

LIST OF TABLES **PAGE NO.**

CHAPTER 1

INTRODUCTION

1.1-DIFFERENT SYNTHESIS ROUTES

1.1.1-SOLID STATE ROUTE:

It is the widely used method for the preparation of polycrystalline solid from the mixture of solid as starting materials. Solids do not react together at room temperature over normal time scales and it is necessary to heat them to a higher temperature often in order to bring the reactions. The factor in which the feasibility and the rate of a solid state reaction includes,the reaction condition, structural properties of reactants, surface area of the solids, their reactivity and thermodynamic free energy change associated with the reaction. A solid state reaction allows the reactants to chemically react in absence of the solvents. In normal reaction technique, scientists need to remove the residual solvent from the resulting product as soon as the reaction has finished. But in this process there is no residual solvent.

1.1.2-AUTO COMBUSTION ROUTE:

It is the self propagating synthesis technique which is started with the triggering of an intensive oxidation-reduction reaction of a little part of dry gel by external energy which gives out huge quantity of heat.The heat makes the reaction continue until the fuel burns out.The sol-gel auto combustion process for spinal ferrite synthesis involves exothermic and self sustaining thermally induced anionic redox reaction gel obtained from aqueous solution containing desired metal salts.The Advantages of this technique includes good chemical homogeneity,high product purity and crystallinity.

1.2-CHARACTERISATION TECHNIQUES

1.2.1-X-RAY DIFFRACTION (XRD):

X ray,like other electromagnetic waves,interacts with the electrons cloud of atom.WhenX rays enter the crystal,each atom acts as diffraction centre and the crystal itself as a whole acts as a three dimensional grating.Due to their shorter wave lengths,X rays are scattered by adjacent atoms in the crystal,which interferes constructively and give rise to diffraction effects.

However it is possible only if the path difference between the rays diffracted by two adjacent atoms is an integral multiple of the wavelength.The diffraction pattern which is obtained tell us much about the internal arrangement of atoms in the crystals.The diffraction condition in crystal is well explained by Bragg's law,

BRAGG'S LAW

In 1912, W.H.Bragg and W.L.Bragg pointed that a consequence of three dimensional periodicity of a crystal is that it can be divided into various sets of equidistant parallel planes containing identical atomic arrangements. They discovered that the geometry of the X ray diffraction is similar to the reflection of light by a plane mirror. It is of course follows that the angle between incident ray and reflected ray is 2θ.Thus the words diffraction and reflection are interchangeable in Bragg's law.

According to Bragg' law if the set atomic planes have an inter planer spacing of 'd' and a monochromatic x ray beam of wavelength λ is allowed to incident on the plane with an angle θ and is reflected back with the same angle then

For constructive interference between the rays 1 and 2 the path differencemust be the integral multiple of wavelength i.e.

$2d\sin\theta=n\lambda$

Where n =0, 1, 2, 3 ... represents the order of reflection.This equation is known as Bragg's law.

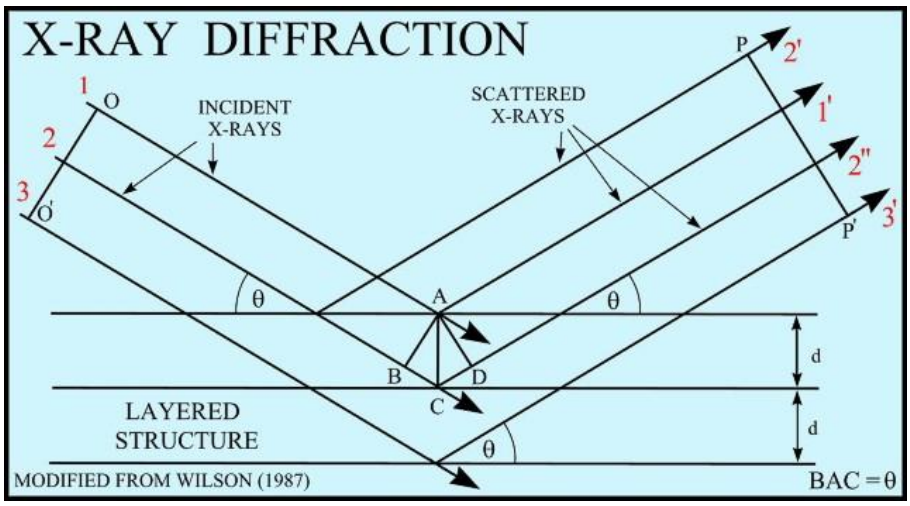

Figure1.1 X-Ray Diffraction

WHY X.RAY?

• Measure the average spacing between layers or rows of atoms.

• Determine the orientation of a single crystal or grain.

• Find the crystal structure of an unknown material.

• Measure the size, shape and internal stress of small crystalline regions.

APPLICATION OF XRD

• XRD is a non-destructive technique.

- It helps To identify crystalline phases and orientation.

• it helps to determine structural properties like Lattice parameters (10^{-4}Å), strain, grain size, epitaxy, phase composition, preferred orientation (Laue) order-disorder transformation, and thermal expansion.

• To measure thickness of thin films and multilayers.

• To determine atomic arrangement.

The **Scherrer equation**, in X-ray diffraction and crystallography, is a formula that relates the size of sub-micrometre particles, orcrystallites, in a solid:

The Scherrer equation can be written as:

$$\tau = \frac{K\lambda}{\beta \cos\theta}$$

τ is the mean size of the ordered (crystalline) domains, K is a dimensionless **shape factor**, with a value close to unity, λ is the X-ray wavelength;β is the line broadening at half the maximum intensity (FWHM), θ is the Bragg angle.

1.2.2-UV VIS SPECTROSCOPY

The measurement of band gap of the materials is very important in semiconductors ,nanomaterial and the solar industries.

The term “band gap” refers to the energy difference between the top of the valance band to the bottom of the conduction band.

We use an UV-VIS spectroscopy to obtain the band gap of the material.

An UV spectrometer is named for the two light sources incorporated into the unit,usually deuterium and tungsten. A UV visible spectrometer is typically used in quantitative determination of the colourless substance in solution ,measuring the transition metal ions and highly conjugated organic compounds. it functions within the spectral range of 200 to 750 nm. The units measure the intensity of light that passes through the sample and compares it with the intensity of light before it passed through the sample.The wavelength of the light is determined after it passes through the sample.The physical quantities T, R and A are measured by using UV-Vis spectrophotometer. The following relationship holds among these measured values.

A + R + T = 1

Usually,in order to consider the absorption properties of a sample from a point of view microscopic physical properties, the bandstructure is used based on the perturbation theory of quantum mechanicsthe ,electronic state, the effective mass of the carrier, and the absorption coefficient α
(cm-1) which is the related to transition step of optical absorption described in transition probality of electrons.

The band gap is found using formula:

$$(\alpha h\nu)^{1/n} = B(h\nu - E_g)$$

Where α is the absorption coefficient

B is a constant

E_g is the band gap

n =1/2(for direct band gap)

n=2(for indirect band gap)

A graph against $(\alpha h\nu)^{1/n}$ and E_g is plotted,the tangent extended to X axis gives the band gap energy.

1.2.3- IMPEDANCE SPECTROSCOPY

Measurement of dielectric constant-

The dielectric constant of the sample is measured using the formula-

$$C_O = A \in_0 / d$$

Where,A=Area of the pellet

d=diameter of the pellet

$\in_o =$ permittivity of free space

Hence, $\in_r = C / C_0$,where C is found from the apparatus.

The dielectric constant is measured at room temperature from the frequency range of 100 Hz to 1 MHz. A frequency vs $\in_r$ curve is plotted.

Impedance Measurement:

Impedance is a sum of the total opposition offered to the current flow in an alternating current circuit, it is made up of two components i.e the ohmic resistance and reactance, and usually represented in complex notation as $Z = R + iX$, where R is the ohmic resistance and X is the reactance.

The resistance(i.e the real part) and the inductance (i.e the imaginary part) is given by Z' and Z" respectively.

Z is given by the instrument itself.

Z'=Zcosθ

Z"=-Zsinθ

Whereθ= phase angle.

AC Conductivity Measurement:

AC conductivity is a measure of a material's ability to conduct an electric current.

It is given by:

$\sigma = Z'/(Z'^2 + Z''^2)(t/A)$,

where,Z’ is real part of the impedance

Z” is the imaginary part

t is the thickness of pellet

A is the area of the pellet

Frequency vs Z’,frequency vs Z” and frequency vs σ curves are plotted at room temperature.

1.2.4-SQUID VSM

The signal of interest in a SQUID VSM instrument is coupled to the SQUID by a superconducting flux transformer comprising of a pick-up loop and an input coil tightly coupled to SQUID.

Owing to flux quantization in superconducting rings, any change in magnetic flux through the pick-up loop due to the signal of interest results in a flow of screening current in the flux transformer coupling magnetic flux through the SQUID loop and the SQUID responds by generating a proportional output voltage. In a conventional SQUID magnetometer, sample is repeatedly transported across a superconducting pick-up loop in the form of a first or second order gradiometer and the SQUID output voltage is recorded as a function of sample position in the form of a flux profile, and the magnetization of the sample is inferred by fitting the measured flux profile to that expected for a point dipole. Since a full flux profile has to be recorded at each value of T and H, measurements over an extended range of T and H tend to take a long time.

A conventional VSM measures the voltage induced in a pick-up loop by Faraday's law of induction as the sample is vibrated in its vicinity, making the measurements relatively faster, although at a slightly poorer sensitivity compared to that offered by a conventional SQUID magnetometer. In a SQUID VSM, sample is fixed at a point where the slope of the flux profile is maximum and is vibrated about this mean position at a low frequency, while the SQUID output is recorded as a function of temperature. Since the full flux profile does not have to be recorded, measurements

over an extended range of T and H can be completed in a relatively short period of time using a SQUID VSM, compared to what is possible with a conventional SQUID magnetometer.

SQUID VSM thus combines the high sensitivity of the SQUID with high speed of measurement of a conventional VSM.

1.3-MAGNETISM

Magnetism has a very ancient history;it is perhaps that aspect os solid state physics that is familiar to all man in the early 800 BC.the three important facts associated with the magnetic materials are :

1-some of the magnetic materials are magnetic even in absence of any magnetic field and become magnetic when a weak magnetic field is applied .

2-some magnetic material looses their initially strong magnetism when they are heated above a certain critical temperature and become comparatively very weakly magnetized.

3-many materials show a magnetic response in a direction opposite to that of the applied field.

The Weak magnetic effects occur in all substanceslike gas, liquid,, solid,but the greater periodicity of atoms in solids leads to stronger cooperative effects.if the interaction of magnetic field is such that the magnetic moments of the atom is aligned,this leads to a very strong magnetic field called as ferromagnetism below a certain temperature known as curie temp (T_c).there are other effects which leads to partially cancelling or complete cancelling of the of the magnetism of different atoms i.e ferrimagnetism and antiferrromagnetism respectively.Ferromagnets become paramagnet above curie temperature.

The magnetic effects in the magnetic materials are due to the atomic magnetic dipoles in the materials.these dipoles result are due to the effective current loops of electrons in atomic orbits,due to this effects of electron spin and from the magnetic moments of atomic nuclei.since all these motions of charged particle,form closed electric current loops ,these are equivalent to magnetic dipoles. When such dipoles are subjected to the external electric field,they experience a torque which tends to align there magnetic

moments in the direction of applied field.The degree of alignment is characterized by the total magnetic moment per unit volume known as *magnetization.*The magnetic moment per unit volume is related to theapplied magnetic field by the relation-M=Xh,where χ is called the magnetic susceptibility of the material.

1.3-TYPES OF MAGNETIC MATERIALS

1.3.1-DIAMAGNETS

A diamagnet is a substance that exhibits negative magnetism even though it is composed of atoms which have no net magnetic moment , it reacts in a special way in the applied magnetic field.

Electons which constitute the closed shell in an atom usually have their own spin and orbital moments which are oriented as a whole in order to cancel net magnetic moment of atom . Thus the mono atomic rare gases like He ,Ne,Ar etc which possess the closed shells electronic structure s are all diamagnetic.diamagnetism is an extremely small and weak effect of magnetism caused by the response of the orbiting electrons to the applied magnetic field in accordance with Lenz's law. The magnetism and susceptibility both are negative for diatomic materials and susceptibility is independent of temperature. Diamagnetic materials reduces the density of lines of forces.

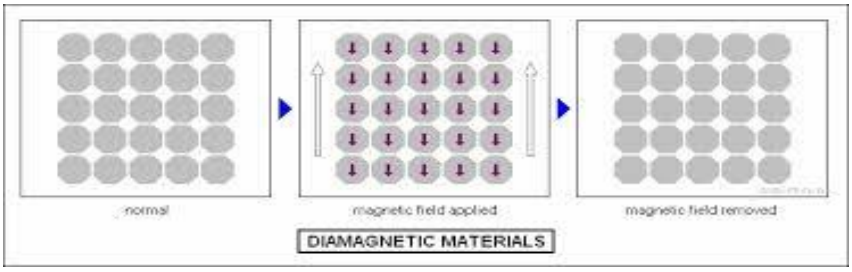

Figure 1.2 Magnetic Moments of a Diamagnetic Material

1.3.2- PARAMAGNETS

There are some materials in which permanent magnetic moments of atoms or ions are acted individually with mutual interaction among them which is randomly distributed,this effect is called paramagnetism. However, in presence of the magnetic field ,the magnetic moments align themselves in the direction of field. If there is no

opposing forces acting ,complete alignment of the magnetic moments can be produced and the specimen as a whole aquires a large magnetization in the direction of the applied field.however the thermal agitation of atoms opposes the tendency and tries to keep the atomic dipoles at random directions .this results in only the partial alignment towards the field direction.Therefore a very weak magnetization and and small susceptibility is present .an increase in temperature therefore decrease the suscpeltibility.Effectively materials with atoms of unpaired spins are paramagnetic.

In paramagnetic substance $\mu > 1$, χ is small,positive and varies inversely with absolute temperature.

The paramagnetic materials obey the curie weiss law,

$$\chi = C/T - \theta$$

Θ is a constant with dimension of temperature.

Paramagnetic materials include manganese, platinum ,tungsten,some members of rare earth group formed by adding and removing electrons to basic atoms thereby creating unpaired electrons.

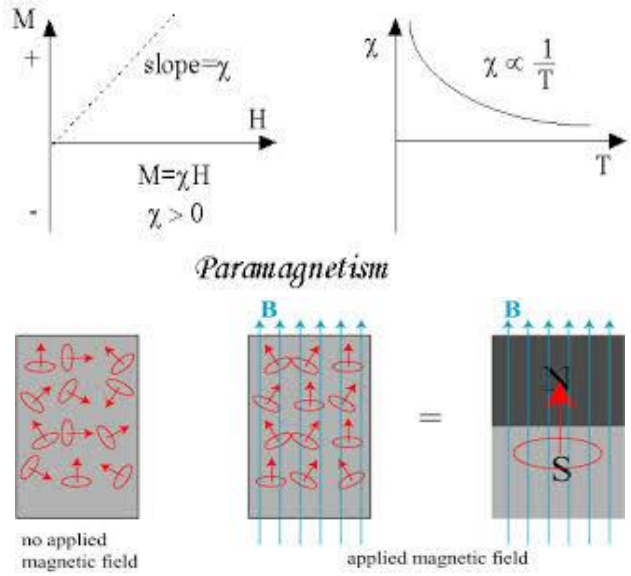

Figure1.3 Paramgnetic Behavior

1.3.3-FERROMAGNETS

Ferromagnets are said to be the permanenet magnet,since it exhibits magnetic property even in the absence of an applied field,however it is found experimentally that the magnetization is increased when an external external magnetic field is applied to the

specimen. Moreover the relationship between B and H is non-linear i.e,ferromagnetic materials exhibits hysteresis.Hysterisis comes from the greek word and refers to the retardation in the response of the material to a change in the applied field.

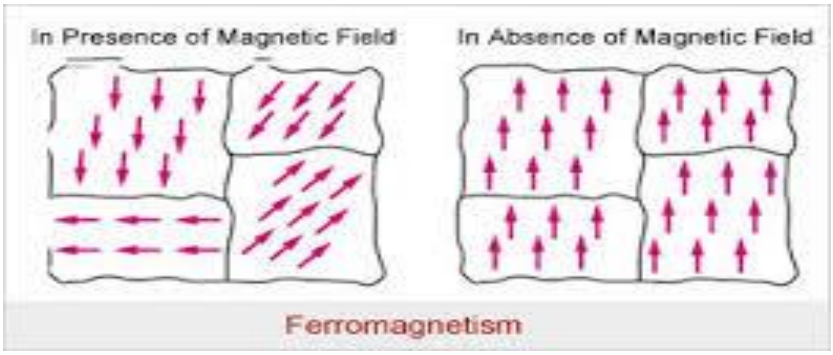

Figure 1.4 Ferromagnetic Behavior

HYSTERISIS LOOP:

In fig 1.5 there is a typical (B-H) diagram for a ferromagnetic material, as the applied field is increased to a positively large value which is large enough to saturate the polarization of the material, B is then reduced to a negative value which is large enough to produce a saturation in reverse direction and than increased to zero once more. A symmetrical closed loop is obtained known as hysteresis .The magnetic induction remaining when the applied field is reduced from saturation to zero is called *remanance,* H_r .The size of the negative field required to reduce the induction to zero is called the *coercivity* H_c.

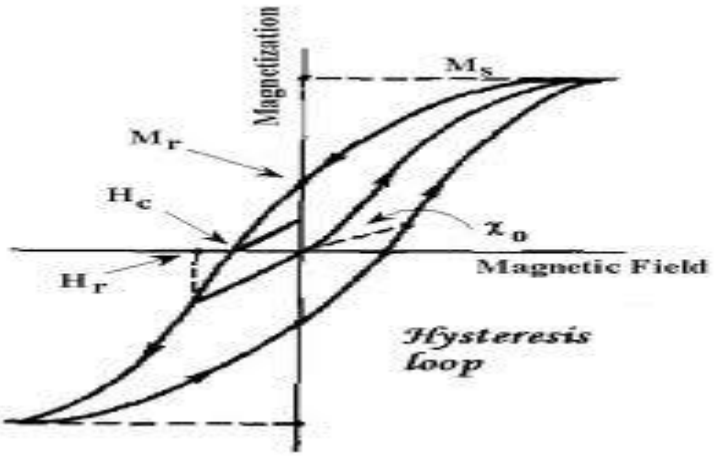

Figure 1.5 Hysteresis Loop

For a given ferromagnetic material,the spontaneous magnetization can occur only below a certain temperature called as curie temperature(T_C),the susceptibility is given by curie-weiss law:

$$\chi = C/(T - T_c)$$

1.3.4 –FERRIMAGNETS

The ferromagnetic material has a property of getting spontaneously magnetized below a certain temperature called as curie temperature which arises due to the non-parallel alignment of atomic magnetic moments. There is an interaction with an unbalance of the two spins systems.The external behavior of ferromagnetic material is similar to the ferromagnetic material,but because of theredifference in the internal structure ,the temperature dependence is quite difference.Ferromagnetic materials are the salts of some of the transition metals particularly which crystallize in the spinel structure.

1.3.5-ANTI FERROMAGNETS

Antiferromagnetism refer to a phenomenon exhibited by some materials in which there is complete magnetic moment cancellation whih occurs as a result of antiparallel coupling of adjacent atoms or ions. The macroscopic solid of an antiferromagnetic material has no net magnetic moment.An antiferromagnet is a special case of a ferrimagnet for which both sub-lattices A and B has equal saturation magnetization.

According to curie weiss law the susceptibility is given by:

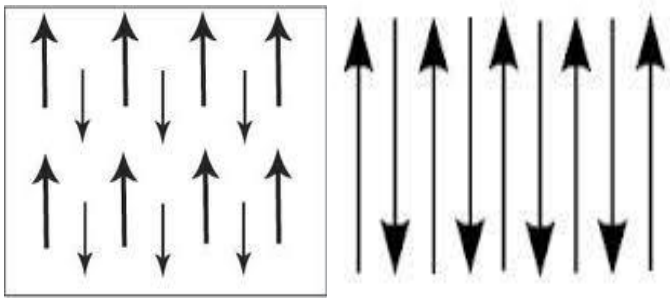

Figure 1.6 Antiferromagnetic material

1.3.6-ANISOTROPIC CRYSTAL

In a single crystal, the physical and mechanical properties often differ with orientation. It can be seen from looking at our models of crystalline structure that atoms should be able to slip over one another or distort in relation to one another easier in some directions than others. When the properties of a material vary with different crystallographic orientations, the material is said to be anisotropic**.**The direction of the ease magnetization of a crystal is the dirction of spontaneous domain magnetization in the demagnetized state. The crystal anisotropy is due mainly to spin-orbital coupling.The magnitude of the crystal anisotropy generally decreases with temperature more rapidly than the magnetization,and vanishes at the curie point.

1.3.7-HARD AND SOFT MAGNETIC MATERIALS

SOFT MAGNETIC MATERIALS

The most widely used permeable materials are iron and iron alloys such as iron – silicon,nickel-iron,etc.these materials are characterized by high electrical resistivity and high permeability under high flux densities they have low cohersive force and are magnetized and demagnetized easily.hencethey are used for transformer course,magnetic switching circuits,and magnetic amplifiers etc.

HARD MAGNETIC MATERIALS

Hard mangnetic materials are used entirelty for their abilty to retain magnetic fields,hence both a large coercive force and high residual induction are desirable to provide and educate magnetic field from the magnet and to retain this field under adverse conditions. The permeability is low and a large magnetic force is necessary to attain saturation magnetization of the materials. The ceramics permanent magnetic materials exhibit this property.

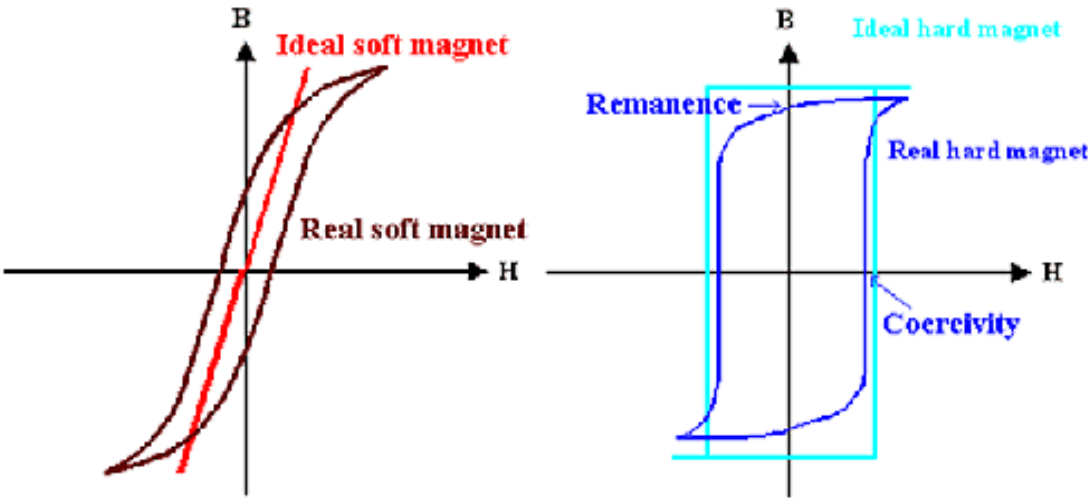

Figure 1.8 Hysteresis Loop Of Hard and Soft Magnetic Material

As hard magnetic materials have potential applications in various fields, so here we concentrating on a well-known M-type hexa-ferriate (hard magnetic material) as $BaFe_{12}O_{19}$ for our present investigation through this project work.

CHAPTER-2

REVIEW ON LITERATURE SURVEY

2.1-STRUCTURE OF $BaFe_{12}O_{19}$

M-type ferrite, $BaFe_{12}O_{19}$, has lattice constants a= 5.89 A˚ and c= 23.19 A˚ in an hexagonal closed packed lattice of oxygen and Ba with Fe in octahedral (12 k,$4f_2$, and 2a), tetrahedral ($4f_1$), and trigonalbipyramidal/hexahedral (2b) sites. The Fe cations are the sole source of magnetic moment: the 12 k,2a, and 2b sites are spin up and $4f_1$ and $4f_2$ sites are spin down, as indicated in Fig.2, where the numbers in the site designations show total number of such sites in the unit cell. The general structure of M type hexaferrite ($AO.6Fe_2O_3$ or $AFe_{12}O_{19}$, where A is a divalent ion such as Ba^{2+}, Sr^{2+}, Pb^{2+}, etc.), which is hexagonal with space group P63/mmc, is constructed from 4 building blocks, namely S, S*, R, and R* . The oxygen atoms are closed packed with the A and Fe ions in the interstitial sites. There are ten layers of oxygen atoms along the c axis and the iron atoms are positioned at five crystallographically different sites. The S (Fe_6O_8) and S* blocks are spinels with 2 oxygen layers and six Fe^{3+} ions. Four of these Fe^{3+} ions are in the octahedral sites with their spins aligned parallel to each other. The remaining two Fe^{3+} ions are in tetrahedral sites and have their spins antiparallel to those that are at the octahedral sites. As for the hexagonal R (AFe_6O_{11}) and R* blocks, they consist of three oxygen layers with one of the oxygen anions replaced with an A ion (A= Ba/Sr/Pb). Each R block contains six Fe^{3+} ions, of which five are in octahedral sites, three having spin up and two having spin down.

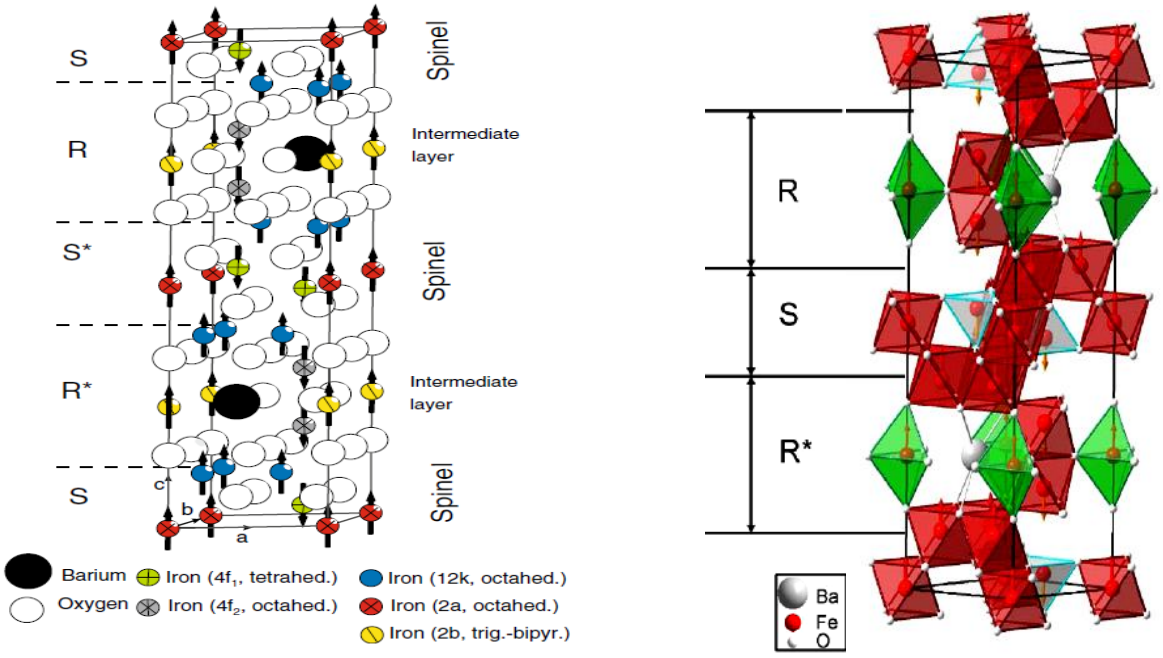

Figure 2.1.*Crystal Structure Of Barium Hexaferrite (2*BaFe$_{12}$O$_{19}$) showing a unit cell and position of ionic sites in the four spinel blocks (SRS*R*) and relative orientation of magnetic moments of Fe^{3+} ions*

polarization. In addition, one of the Fe^{3+} ions is coordinated with five O^{2-} anions and has spin up polarization. The Fe atoms at the 2a site are octahedrally coordinated with equal Fe–O distances, while the octahedrally coordinated Fe ions at $4f_2$ and 12 k sites have different Fe–O interatomic distances, from about 1.85–2.37 A˚´ Of the twelve Fe^{3+} ions of the formula unit, the Fe atoms at $4f_1$ sites are tetrahedrally coordinated by oxygen, while the Fe atoms at 2b sites are coordinated by five oxygen ions. There are also short Fe–Fe distances in the structure, and at $4f_2$ sites this Fe–Fe distance is about 2.7 A˚. The Fe ions at 12 k sites form a network with every Fe connected to four other Fe ions in the same layer. In terms of spin, in R block one ion in the 2b layer is up state and two octahedral ions are down state, and in S block seven octahedral ions up state and two tetrahedral ions down state.

2.2-ORIGIN OF MAGNETISATION IN $BaFe_{12}O_{19}$

In the structure, each Fe^{3+} ion contributes 5μB to the magnetic moment at absolute zero, the total magnetization at zero temperature can be calculated knowing that eight Fe^{3+} ions are in the spin upstate, and four are in spin down state resulting in four net

spin up Fe^{3+} ions. Therefore, the net magnetization per molecular unit is (1- 2+ 7- 2) * 5μB= 20μB (One Ba ion per molecular unit)**.**

Table-2.1- Number of ions per unit formula, coordination and spin direction for the Fe^{3+}cationsublattices of M-type BaM

Lattice sites per unit formula	Coordination	Number of Fe^{3+} ions	Block	Spin direction
12k	Octahedral	6	R-S	Up↑
2b	Trigonal–bipyramidal	1	R	Up↑
$4f_2$	Octahedral	2	R	Down↓
$4f_1$	Tetrahedral	2	S	Down↓
2a	Octahedral	1	S	Up↑

2.3-DIFFERENT PROPERTIES OF $BaFe_{12}O_{19}$

Barium hexaferrite, with its chemical formula $BaFe_{12}O_{19}$ (denoted as BF), is the best-known representative of the hexaferrite family which is used extensively as a relatively low cost ceramic permanent magnet. BF is one of the most important hard magnetic materials, widely used in permanent magnets, magnetic recording media, and microwave applications, due to its fairly large magnetocrystalline anisotropy, high Curie temperature, relatively large magnetization, as well as excellent chemical stability and corrosion resistance. BFcrystallizes in a hexagonal structure with 64 ions per unit cell on 11 different symmetry sites. The 24 Fe^{3+}atoms are distributed over five distinct sites: three octahedralsites (12k, 2a, and $4f_2$), one tetrahedral site($4f_1$), and one bipyramidal site (2b). Its crystal structure is the so-called magnetoplumbite structure, which can be described as a stacking sequence of the basic blocks S and R.BaM has 20 μB and this gives it a high saturation magnetisation of 72 A m^2 kg^{-1} and a high Curie temperature of 450 ^oC. It also has a high anisotropy constant, $K_1 = 3.3 * 10^6$ erg cm^{-3}. The reported H_c values of BaM prepared from standard ceramic methods is around 159–255 kA m^{-1}**.**

CHAPTER 3

SYNTHESIS OF $BaFe_{12}O_{19}$

3.1-WITHOUT PRECAUTION(SAMPLE-1)

3.1.1-FLOW CHART

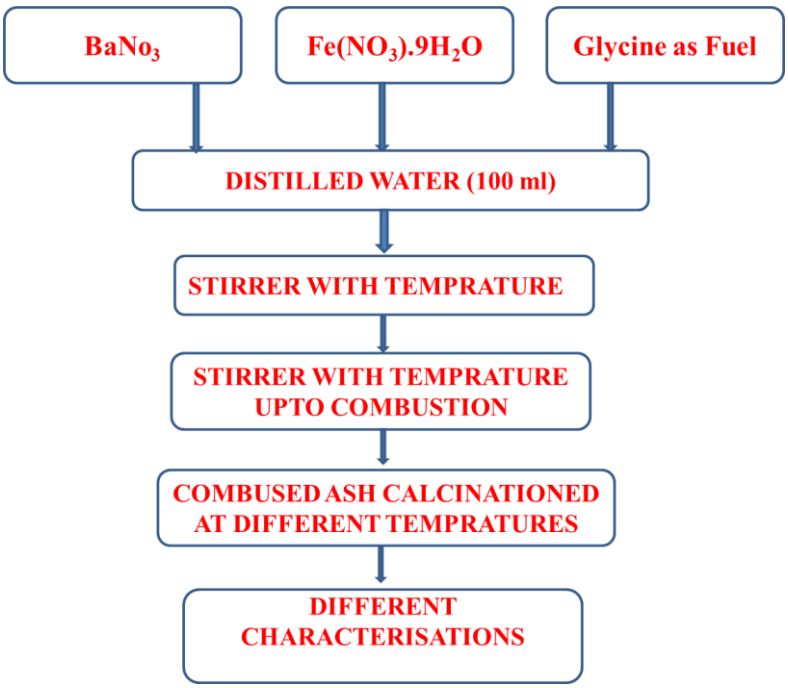

3.1.2-XRD (At Different Calcinations Temperatures)

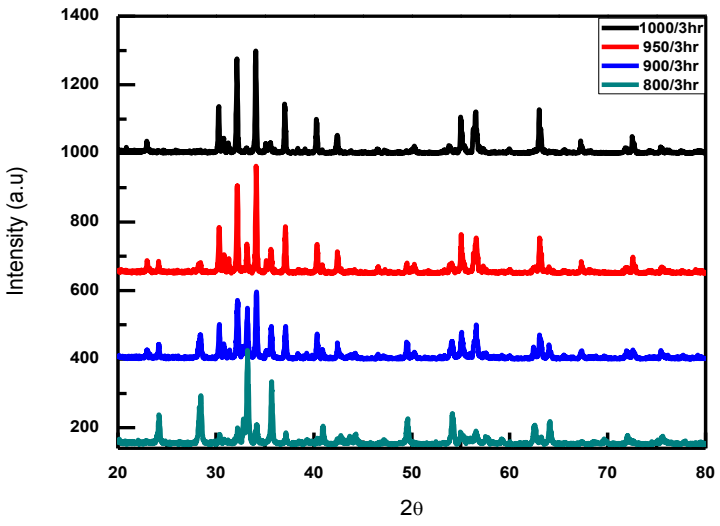

Figure-3.1: Without Precaution (Sample-1)

From the XRD data (Fig.3.1) for Sample-1 pure phase formed at 1000/3hr

3.1.3-Particle SizeMeasurement (Table-3.1)

No.	Position(2θ)	FWHM(2θ)	β	Cosθ/2	τ(in nm)	Average particle size(nm)
1	22.9669	0.1181	0.00206	0.97998	71.7	54.2
2	30.2823	0.1181	0.00206	0.96529	72.79	
3	30.7944	0.1771	0.00309	0.96411	48.6	
4	31.2731	0.1181	0.00206	0.96299	72.96	
5	32.1426	0.0984	0.00172	0.96092	87.76	
6	33.1343	0.2362	0.00412	0.95849	36.65	
7	34.051	0.1574	0.00275	0.95617	55.13	
8	35.0888	0.1181	0.00206	0.95348	73.69	
9	35.5704	0.1574	0.00275	0.95221	55.36	
10	37.0417	0.0984	0.00172	0.94821	88.93	

3.2-WITH PRECAUTION(Ph control upto 7)(SAMPLE 2)

3.2.1-FLOW CHART(SYNTHESIS PROCESS)

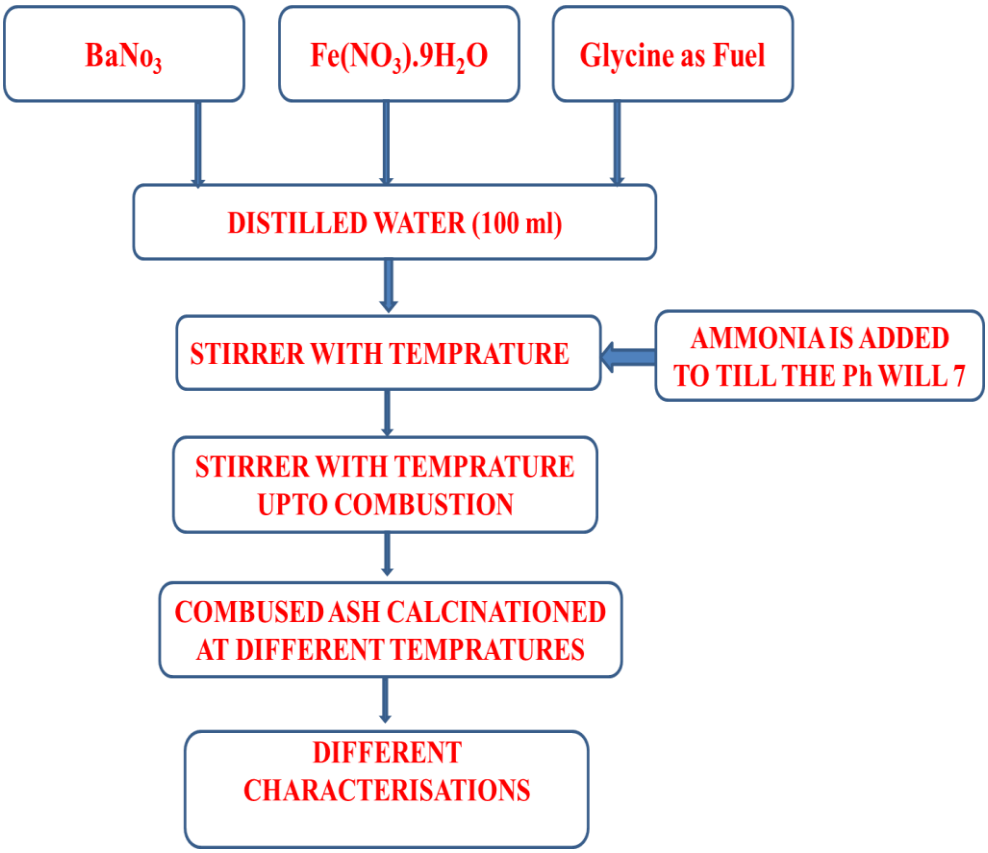

3.2.2-XRD (At Different Calcinations Temperatures)

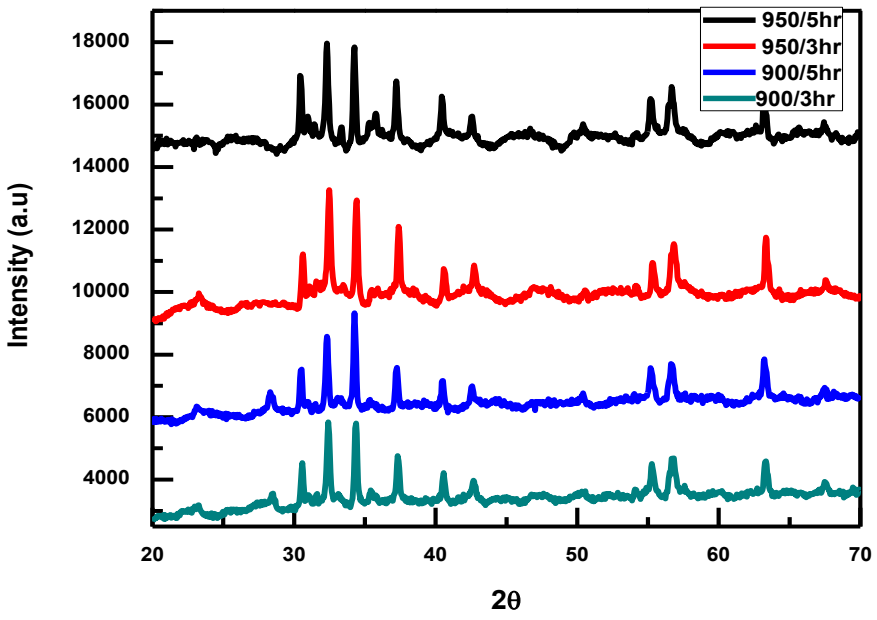

Figure-3.2 With Precaution (Ph Control Upto 7)

From the XRD data (Fig.3.2) for Sample-2 pure phase formed at 950/3hr

3.2.3-Particle Size Measurement:(Table-3.2)

No.	*Position(2θ)*	*FWHM(2θ)*	*β*	*Cosθ/2*	*τ(in nm)*	*AverageParticle Size (nm)*
1	23.298	0.3936	0.00687	0.9794	21.52	
2	30.6188	0.1968	0.00343	0.96451	43.71	
3	31.5822	0.1476	0.00257	0.96226	58.42	
4	32.4891	0.1968	0.00343	0.96008	43.91	**40.18**
5	34.4116	0.1968	0.00343	0.95525	44.14	
6	35.4693	0.1968	0.00343	0.95248	44.27	
7	37.4043	0.1476	0.00257	0.9472	59.35	
8	40.5952	0.1968	0.00343	0.9379	44.95	
9	42.7239	0.1968	0.00343	0.9313	45.27	
10	46.9218	0.7872	0.01373	0.91733	11.49	

3.3-WITH PRECAUTION(USING HNO_3)(SAMPLE-3)

3.3.1-FLOW CHART (SYNTHESIS PROCESS)

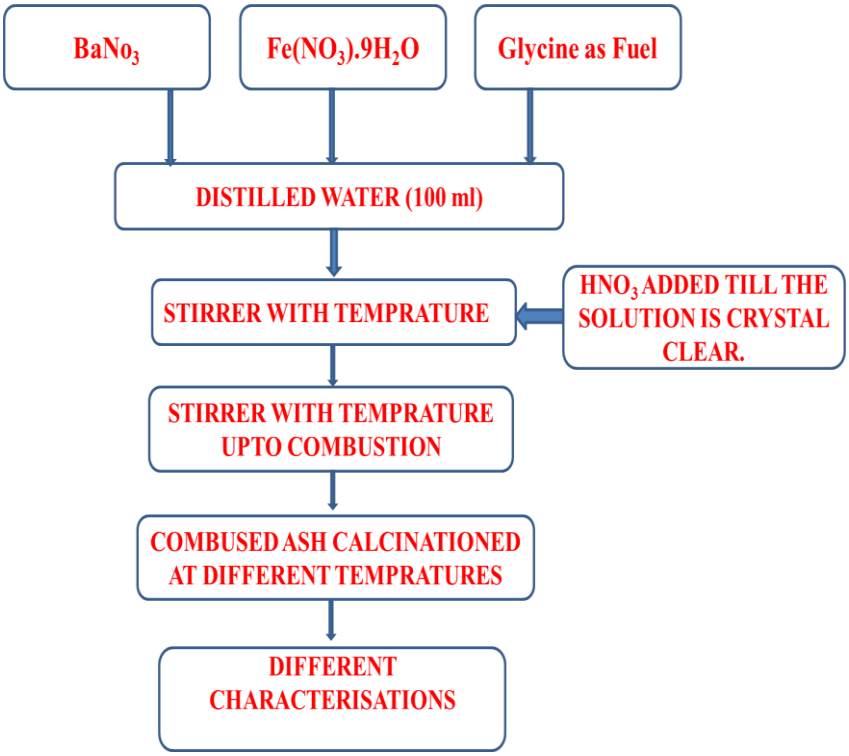

3.3.2-XRD(different calcinations temperatures)

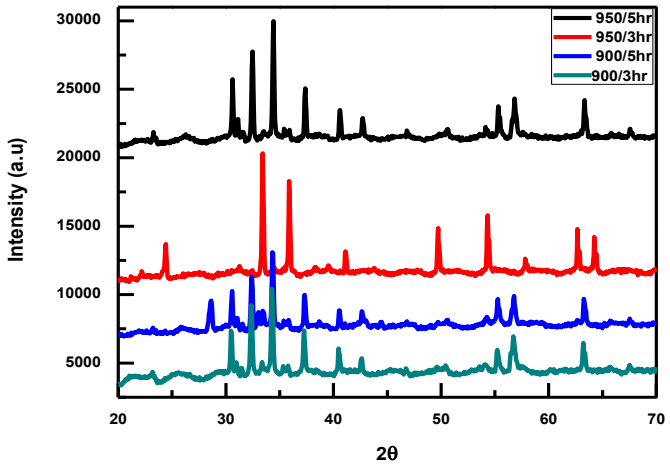

Figure-3.3 With Precaution (Using HNo_3) (Sample-3)

From the XRD data (Fig.3.3) for Sample-3 pure phase formed at 950/5hr

3.3.3- Particle Size Measurement:(Table-3.3)

No.	Position(2θ)	FWHM(2θ)	β	Cosθ/2	Particle size(in nm)	Average particle size(in nm)
1	23.2757	0.1476	0.00257	0.97944	57.4	
2	26.2644	0.984	0.01717	0.97385	86.59	
3	30.6306	0.1968	0.00343	0.96449	43.71	
4	31.1174	0.1476	0.00257	0.96336	58.36	
5	31.6413	0.1476	0.00257	0.96212	58.43	**52.79**
6	32.4777	0.1968	0.00343	0.9601	43.91	
7	34.4201	0.1476	0.00257	0.95523	58.85	
8	35.4257	0.1476	0.00257	0.95259	59.01	
9	35.9085	0.1476	0.00257	0.9513	59.09	
10	37.3803	0.1968	0.00343	0.94727	44.51	

Particle Size Comparison Table 3.4

Preparation method	*Calcination temp*	*Particle size*
Without precaution	1000°C/3hrs	54.2
With ammonia	950°C/3hrs	40.18
With HNO3	950°C/5hrs	52.79

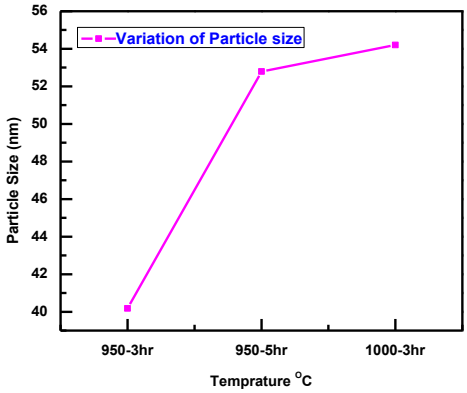

Figure 3.4 Particle Size Comparision

3.4 Result and Discussion:

The X-ray diffraction analysis confirms the formation single phase formation of $BaFe_{12}O_{19}$ for all three precaution roots. It was found that the calcined temperature for Sample-1 is 1000°C/3hr, for Sample-2 950°C /3hr and for Sample-3 950°C/5hr. From the particle size measurement by using Scherer's formula shows that the average particle size are54.2nm, 40.18nm and 52.79nm for Sample-1, Sample-2 and Sample-3 respectively. From the variation of particle size it can conclude that as calcined temperature and time duration increases the corresponding particle size also increases.

CHAPTER 4

UV VISIBLE SPECTROSCOPY STUDY

All the pure phase formation powders gone for Uv-Visible study

4.1-BAND GAP MEASUREMENT AND ANALYSIS-

The band gap is calculated using UV-VIS spectrometer which givesWavelength(λ) and reflectance(R) from which we can calculate the band gap energy using relation: $(\alpha h\nu)^{1/n} = B(h\nu - E_g)$ (n-0.5-for direct band gap), $\nu = c/\lambda$,A=(100-R), hν-Energy, α =log A and B is a constant.

Band gap energy for different samples are as follows:

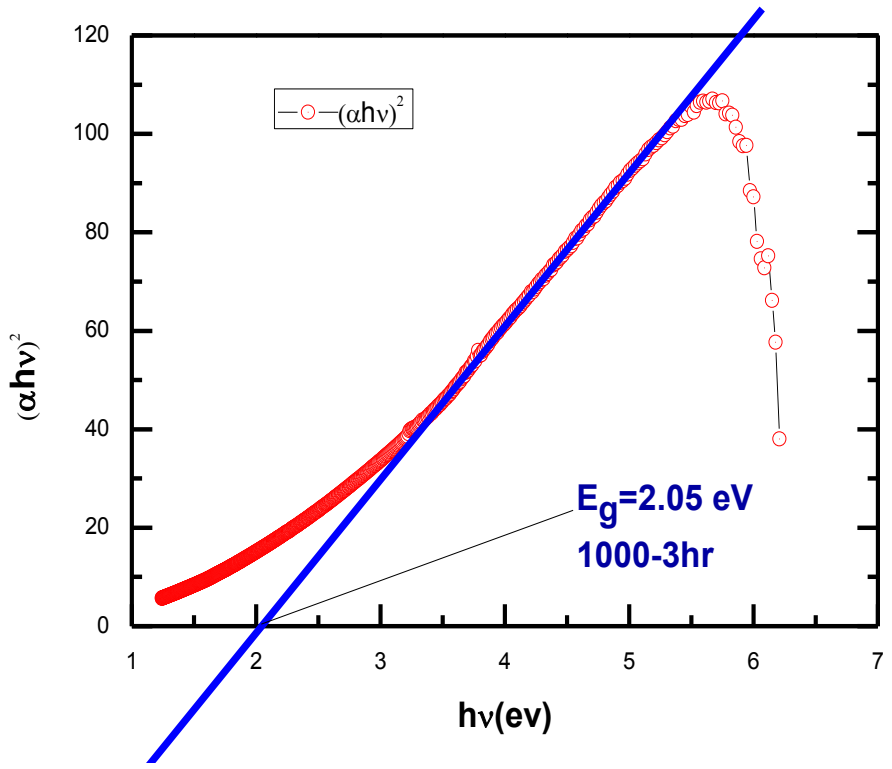

Figure-4.1 Without precaution(1000°C/3 hrs)

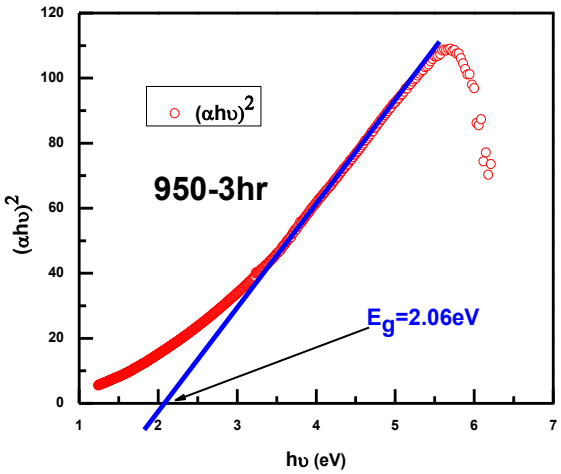

Figure-4.2 With Ammonia(950°C/3 hrs)

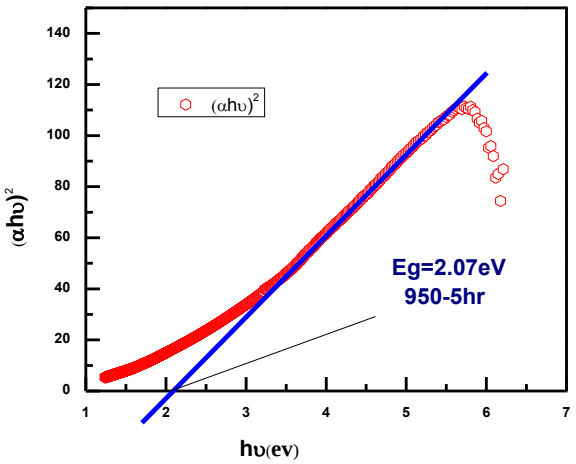

Figure-4.3With HNO_3 (950°/5 hrs)

Comparative study of band gap energies:

Preparation method	**Band Gap E_g(ev)**
Without precaution(1000°C/3hrs)	2.05
With ammonia(950°C/3hrs)	2.06
With HNO_3 (950°C/5 hrs)	2.07

4.2 Result and Discussion:

The calculated band gap for all the samples from UV-Visisble spectroscopy data shows that, all the samples have approximately same band gap energy.

CHAPTER-5

DIELELECTRIC,IMPEDANCE AND CONDUCTIVITY STUDIES

All pure phase formed powders sintered at same temperature.From the XRD data (Fig-5.1, Fig-5.2 and Fig-5.3) of all pellets, it is clear that only 950°C/5hrs pellethas pure phase came and for other two not appeared.So that 950°C/5hrs considered for room temperature dielectric,impedance and conductivity study.

XRDOf Sample-1 (Pellet Sintered at1000°C/3hrs)

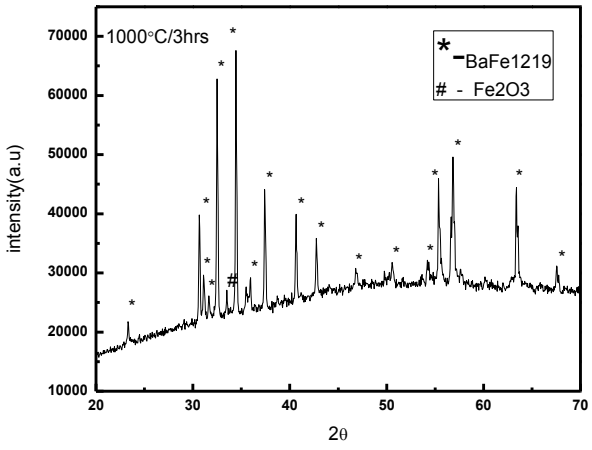

Figure-5.1

XRD Of Sample-2 (Pellet Sintered at950°C/3 hrs)

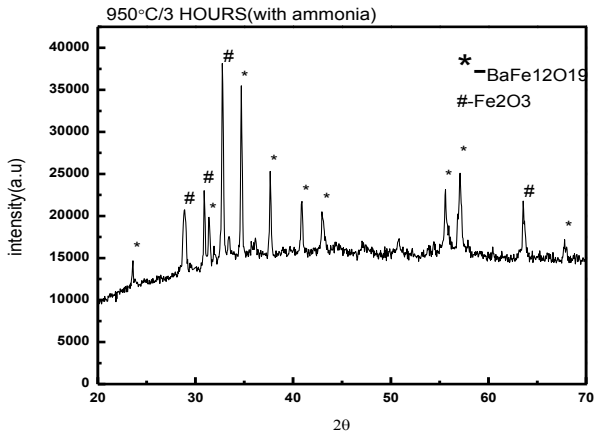

Figure- 5.2

XRD Of Sample-3 (Pellet Sintered at 950°C/5 hrs)

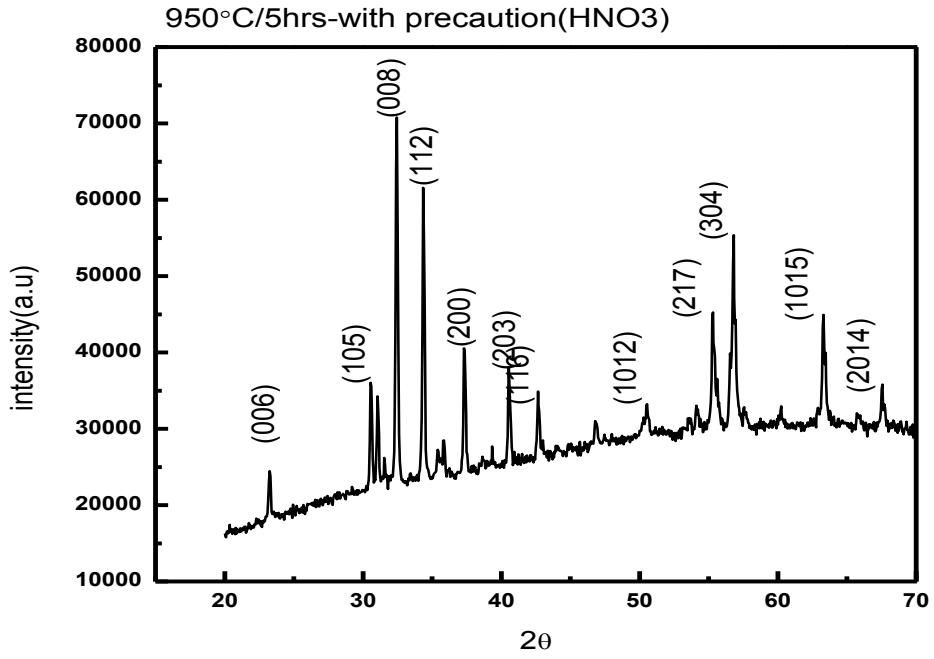

Figure-5.3

Table -5.1(Crystal Structure Information of Pellet Sintered at 950°C/5 hrs from JCPDS File No 07-0276)

Crystal system:	**Hexagonal**
Space group:	P63/mmc
Space group number:	194
LATTICE PARAMETERS	
a (Å):	**5.8760**
b (Å):	**5.8760**
c (Å):	**23.1700**
α(°):	**90.0000**
β (°):	**90.0000**
γ **(°):**	**120.0000**

5.1 Dielectric Property:

Generally, dielectric property of a material depends upon polarization occurs inside the material in different frequency and temperature ranges.

The polarization in ferrites is through a mechanism similar to the conduction process. By electron exchange between Fe^{2+} and Fe^{3+}, the local displacement of electrons in the direction of the applied field occurs and these electrons determine the polarization. The decrease in the dielectric constant with increasing frequency is explained to be due to the decrease of polarization of the dipoles when electric field propagates with high frequency. In other words, beyond a certain frequency of electric field the electron exchange does not follow the alternating field. The large value of dielectric constant at lower frequency is due to the predominance of species like Fe^{2+} ions, oxygen vacancies, grain boundary defects, etc., while the decrease in dielectric constant with frequency is natural because of the fact that any species contributing to polrizability is found to show lagging behind the applied field at higher and higher frequencies.

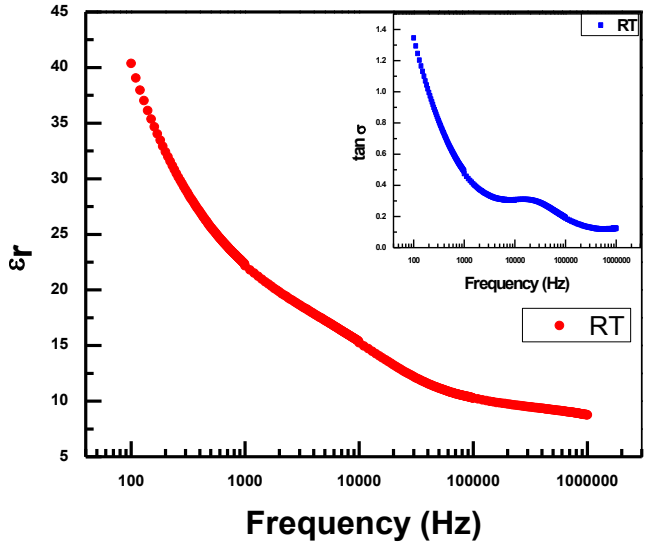

Figure-5.4: Frequency Vs Dielectric Constant and Lossat room temperature

From the Fig-5.4 it can conclude that dielectric constant is decreasing with increasing frequency which is typical dielectric behaviour of a ferrite. The larger value of dielectric constant at lower frequencies is due to the all contribution (atomic,

electronic, ionic and interfacial polarisation). As frequency increases the contribution from the space charge and orientation polarisation reduces so dielectric constant decreases.

5.2 Dielectric Loss Tangent:

The energy loss is usually characterized by the dielectric loss tangent or tanσ. Dielectric loss arises when there is polarization lag behind the applied alternating field which is due to the impurities and imperfections in the crystal. The plots of dielectric loss versus frequencies for sintered Barium ferrite at room temperature are shown in inset of Fig-5.4. It is noticed that the dielectric loss for sample is greater at lower frequencies and decreases rapidly with the increase in frequency. According to phenomenological Koop's theory, this is explained on the basis of the fact that in the low frequency region, where the resistivity is high and the grain boundary effect is dominant, more energy is needed for electron exchange between $Fe^{2+}$and Fe^{3+}ions, as a result the loss is high. In the high frequency region, when the resistivity is low and grains themselves have a dominant role, a small energy is required for electron transfer between the two Fe ions at the different sites.

5.3 Impedance Analysis:

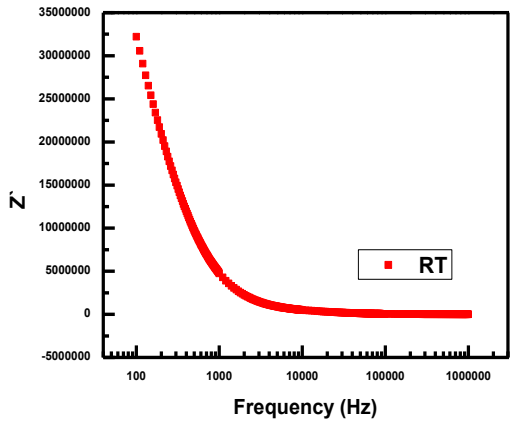

Figure-5.5: Frequency dependency Real(Z_{Re}) Impedance

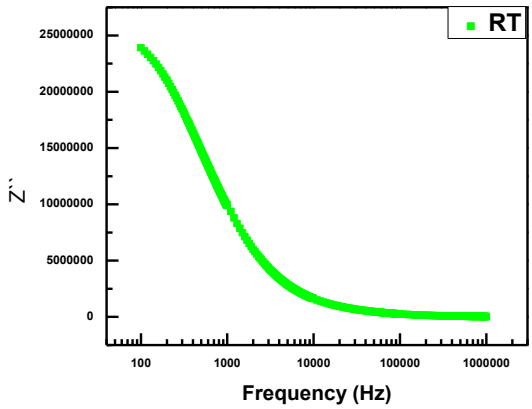

Figure-5.6: Frequency dependency Imaginary (Z_{Im}) part

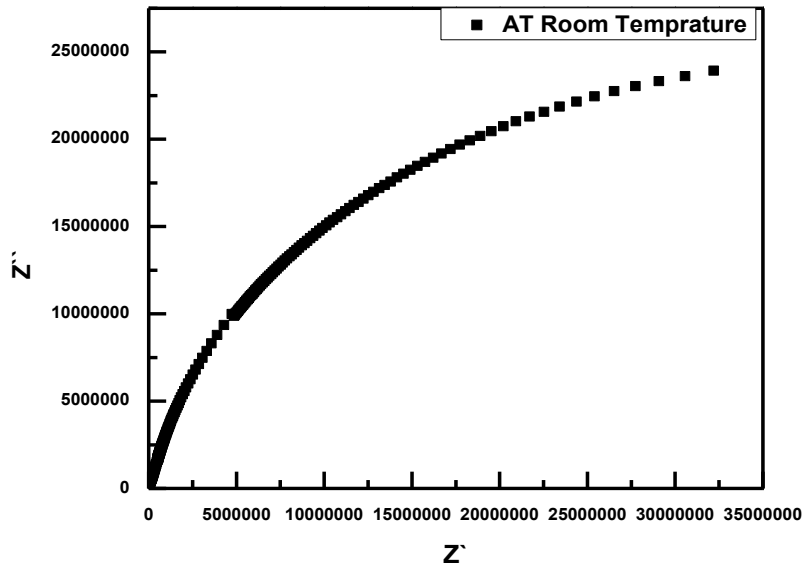

Figure-5.7: Nyquist plot (Z_{Re} versus Z_{Im})at room temperature

The Fig-5.5 and Fig-5.6 shows the variation of Real [Z_{Re}(Z`)] and Imaginary part [$Z_{Re}$(Z`)] of impedance values with frequency at room temperature. The observed behaviour of Z`and Z`` with frequency of the sample says that both the Z`and Z`` are decreasing with increasing of frequency. The Z_{Re} is related to the sample electric resistance and imaginary part of the impedance (Z_{Im}) with frequency suitable to evaluate the relaxation frequency. It is observed from Fig-5.6 that there is absence of dielectric relaxation at room temperature as there is on peak observed.

It is well known that complex impedance spectroscopy is an important tool for study the electrical properties of ferrites since impedance of the grains can be separated from other impedance sources, such as impedance of electrodes and grain boundaries. Generally, two semicircles are observed in the Cole–Cole plots of the sample ferrite powders between the frequency range 100 Hz and 1 MHz.The Fig.5.7 shows the complex impedance (Nyquist) plot of the investigated sample.This plot indicates the presence of only bulk resistance for the sample and the grain boundary resistance is negligibly small as no second semi-circle is observed.

Similarly, as only one semicircle appears in Nyquist plot it can suggest that a predominant conduction is through the grain boundary volume and contribution from the grain is not well resolved in these samples. So, it is therefore concluded that the conductivity for this sample is mainly due to the grain boundary contribution.

5.4-MODULUS ANALYSIS:

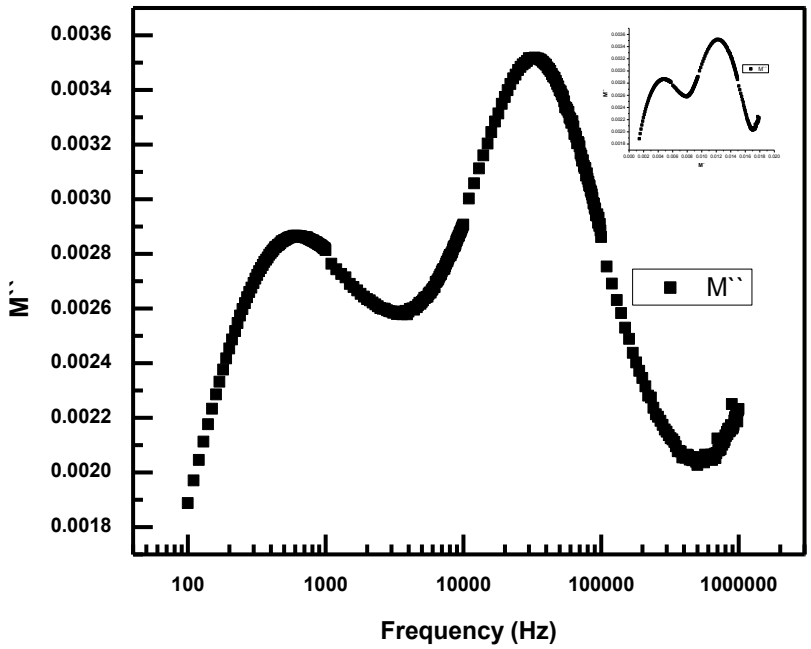

Figure-5.5 M`` (Complex Modulus) Vs Frequency

The Fig-5.5 shows the variation of M`` (Complex Modulus) Vs frequency, here there are two peaks appears but these peaks are absent in cole-cole plot. So that it confirms that both grain and grain boundary contribution are present in this material.

5.5 Conductivity Analysis:

The conductivity vs frequency representation is a most prominent representation to relate the macroscopic measurement to the microscopic movement of the charge carriers. From Fig-5.8 it can confirms that, in case of $BaFe_{12}O_{19}$ a dc plateau appears in the low frequency region and an increase of the conductivity with the increase of the frequency as like a typical behaviour of ionic materials.

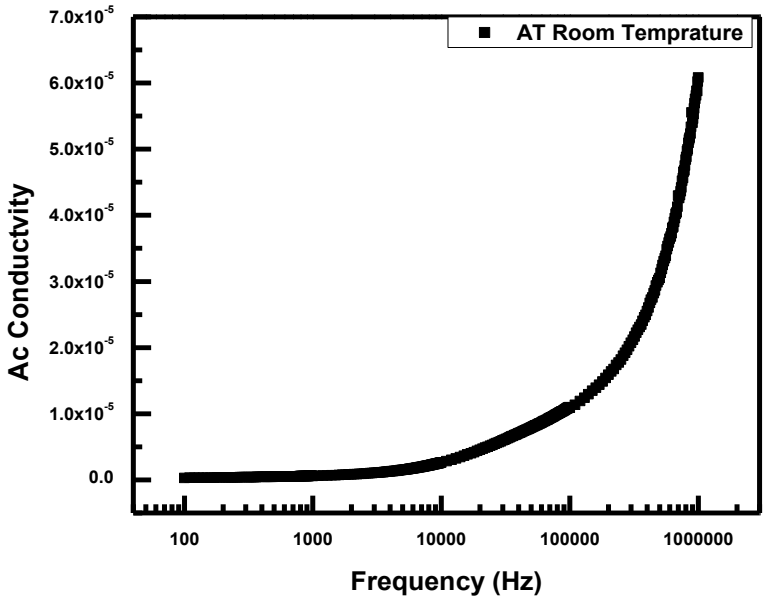

Figure-5.8: Frequency dependency of AC conductivity at room temperature

CHAPTER 6

CONCLUSIONS

We have prepared $BaFe_{12}O_{19}$ using sol–gel auto combustion technique considering three precautions. The X-ray diffraction analysis confirms the formation of single phase of $BaFe_{12}O_{19}$ for all three precaution roots. Using Scherer's formula, the crystallite size of $BaFe_{12}O_{19}$ is calculated, it was found that the average particle size are 54.2nm, 40.18nm and 52.79nm for Sample-1, Sample-2 and Sample-3 respectively. The measured band gap of all three samples from UV Visible spectroscopy data were approximately 2.0eV. From room temperature dielectric spectroscopy of Sample-3, we concluded that dielectric loss of $BaFe_{12}O_{19}$ decreases with increase in frequency. Dielectric constant of $BaFe_{12}O_{19}$ also decreases with increase in frequency and the conductivity increases with increase in frequency. The real and imaginary Impedance of $BaFe_{12}O_{19}$ decreases with increase in frequency. From the cole-cole plot it is concluded that only grain boundary effect present at room temperature.

The modulus vs frequency plot clarifies the presence of both grain and grain boundary contribution to the conduvtivity of the material.

REFERANCES

1-Introduction To Magnetic Materials By B.D Cullity
2-Solid states by S.O PILLAI
3-Introduction to solid states by KITTEL
4-Temperature and frequency characteristics of low-loss MnZn ferrite in a wide temperature range
5-J. Appl. Phys. **109**, 106103 (2011); 10.1063/1.3583551Influence of microstructure on permeability dispersion and power loss of NiZn ferrite
6-J. Appl. Phys. **103**, 093903 (2008); 10.1063/1.2908202Effects of grain size on the residual loss of Mn–Zn ferrites
7-J. Appl. Phys. **91**, 7619 (2002); 10.1063/1.1447506Highly resistive grain boundaries in doped MnZn ferrites for high frequency power supplies
8-J. Appl. Phys. **82**, 333 (1997); 10.1063/1.365817Analysis of eddy current loss in Mn–Zn ferrites for power supplies
9-J. Appl. Phys. **81**Direct correlation between ferrite microstructure and electrical resistivity
10-J. Appl. Phys. **101**, 104912 (2007); 10.1063/1.2735400The magnetic properties of plasma-sprayed thick-film manganese zinc ferrite (MZF) and nickel iron alloy(Permalloy) composites
11-J. Appl. Phys. **99**, 08M915 (2006); 10.1063/1.2171956Influence of grain size and structural changes on the electrical properties of nanocrystalline zinc ferrite
12-J. Appl. Phys. **92**, 2770 (2002); 10.1063/1.1498883Line width of manganese–zinc ferrite polycrystals with oxygen partial pressure
13-J. Appl. Phys. **83**, 6873 (1998); 10.1063/1.367829
Highly resistive grain boundaries in doped MnZn ferrites for high frequency power supplies
14-J. Appl. Phys. **82**, 333 (1997); 10.1063/1.365817
15-Journal of Alloys and Compounds 545 (2012) 225–230
Temperature dependent magnetic and dielectric properties of M-type hexagonal $BaFe_{12}O_{19}$ nanoparticles**J. Krishna murthy a, C. Mitra b, S. Ramc, A. Venimadhav**
16-Impedance spectroscopy analysis of $BaFe_{12}O_{19}$ M-type hexaferrite
Obtained by ceramic method**Ronaldo RibeiroCorreˆab, Carlos William de AraujoPaschoala**